

### **OPEN ACCESS**

EDITED BY Shinya Iwasaki, University of Bremen, Germany

REVIEWED BY
Saverio Bartolini Lucenti,
University of Florence, Italy
Vivi Vajda,
Swedish Museum of Natural History,
Sweden

\*CORRESPONDENCE
Fabiany Herrera,

☐ fherrera@fieldmuseum.org

RECEIVED 05 April 2023 ACCEPTED 23 June 2023 PUBLISHED 14 July 2023

#### CITATION

Herrera F, Hotton CL, Smith SY, Lopera PA, Neander AI, Wittry J, Zheng Y, Heck PR, Crane PR and D'Antonio MP (2023), Investigating Mazon Creek fossil plants using computed tomography and microphotography. Front. Earth Sci. 11:1200976. doi: 10.3389/feart.2023.1200976

### COPYRIGHT

© 2023 Herrera, Hotton, Smith, Lopera, Neander, Wittry, Zheng, Heck, Crane and D'Antonio. This is an open-access article distributed under the terms of the Creative Commons Attribution License (CC BY). The use, distribution or reproduction in other forums is permitted, provided the original author(s) and the copyright owner(s) are credited and that the original publication in this journal is cited, in accordance with accepted academic practice. No use, distribution or reproduction is permitted which does not comply with these terms.

# Investigating Mazon Creek fossil plants using computed tomography and microphotography

Fabiany Herrera <sup>1</sup>\*, Carol L. Hotton <sup>2,3</sup>, Selena Y. Smith <sup>4</sup>, Paula A. Lopera <sup>5</sup>, April I. Neander <sup>6</sup>, Jack Wittry <sup>7</sup>, Yuke Zheng <sup>1,8,9</sup>, Philipp R. Heck <sup>1,8,9</sup>, Peter R. Crane <sup>10,11</sup> and Michael P. D'Antonio <sup>1</sup>

<sup>1</sup>Earth Sciences, Negaunee Integrative Research Center, Field Museum of Natural History, Chicago, IL, United States, <sup>2</sup>National Center for Biotechnology Information, National Library of Medicine, National Institutes of Health, Bethesda, MD, United States, <sup>3</sup>Department of Paleobiology, National Museum of Natural History, Smithsonian Institution, Washington, DC, United States, <sup>4</sup>Department of Earth and Environmental Sciences and Museum of Paleontology, University of Michigan, Ann Arbor, MI, United States, <sup>5</sup>Smithsonian Tropical Research Institute, Panama, Panama, <sup>6</sup>Department of Organismal Biology and Anatomy, The University Chicago, Chicago, IL, United States, <sup>7</sup>Gantz Family Collections Center, Field Museum of Natural History, Chicago, IL, United States, <sup>8</sup>Robert A. Pritzker Center for Meteoritics and Polar Studies, Negaunee Integrative Research Center, Field Museum of Natural History, Chicago, IL, United States, <sup>9</sup>Department of the Geophysical Sciences, The University of Chicago, Chicago, IL, United States, <sup>9</sup>Oepartment of the Geophysical Sciences, The University of Chicago, Chicago, IL, United States, <sup>9</sup>Oepartment of the Geophysical Sciences, The University of Chicago, Chicago, IL, United States, <sup>9</sup>Oepartment of the Geophysical Sciences, The University of Chicago, Chicago, IL, United States, <sup>9</sup>Oepartment of Environment, Yale University, New Haven, CT, United States, <sup>10</sup>Oak Spring Garden Foundation, Upperville, VA, United States

More than 20.000 siderite concretions from the Mazon Creek area of northern Illinois, United States are housed in the paleobotanical collections of the Field Museum. A large proportion contain fossil plants of Middle Pennsylvanian age that often have excellent three-dimensional morphology and sometimes anatomical detail. Approximately eighty plant taxa have been recognized from the Mazon Creek Lagerstätte, but few have been studied in detail, and in some cases the systematic affinities of these fossils need reevaluation. The three-dimensional (3D) preservation of Mazon Creek fossil plants makes them ideal candidates for study using x-ray micro-computed tomography (µCT), and here we apply these techniques to more accurately reconstruct the morphology of specimens of Tetraphyllostrobus Gao et Zodrow and Crossotheca Zeiller. The mineralogical composition of the fossil plant preservation was studied using elemental maps and Raman spectroscopy. In-situ spores were studied with differential interference contrast, Airyscan confocal super-resolution microscopy, and scanning electron microscopy, which reveal different features of the spores with different degrees of clarity. Our analyses show that  $\mu CT$  can provide excellent detail on the threedimensional structure of Mazon Creek plant fossils, with the nature of associated mineralization sometimes enhancing and sometimes obscuring critical information. Results provide guidance for selecting and prioritizing fossil plant specimens preserved in siderite concretions for future research.

### KEYWORDS

Paleozoic, *Tetraphyllostrobus*, *Crossotheca*, micro-computed tomography, MeshLab, differential interference contrast, airyscan confocal superresolution microscopy

### 1 Introduction

The Paleozoic Mazon Creek Lagerstätte is one of the richest fossil assemblages and many thousands of specimens preserved in sideritic concretions have been recovered from the Francis Creek Shale of the Carbondale Formation in the Illinois Basin, United States, which is of Moscovian (~307-311 Ma), Middle Pennsylvanian age. The concretions preserve impressions, casts, and molds of a wide variety of organisms from a broad spectrum of estuarine marine to freshwater environments (Johnson and Richardson, 1966; Nitecki, 1979; Baird et al., 1985; 1986; Clements et al., 2019). The Mazon Creek biota includes many terrestrial animals and plant remains (e.g., Wittry, 2006; 2020) that were evidently washed into coastal and marine depocenters suitable for the formation of siderite concretions in the Mazonian delta (e.g., Cotroneo et al., 2016; McCoy et al., 2016; Clements et al., 2019). Fossils in the concretions exhibit exquisite preservation which reflects the early formation of the nodules prior to significant sediment compaction and decomposition. Fossil metazoans often have the remains of soft tissues preserved. Fossil plants often contain spores (e.g., Drinnan and Crane, 1994) and also have excellent details of external morphology, which is sometimes complemented by the preservation of anatomical details (Drinnan et al., 1990). Among the many metazoans from the deposit are fossil jellyfish, polychaete worms, and the "Tully Monster" (Tullimonstrum gregarium) (Johnson and Richardson, 1966; Richardson, 1966). The latter has been studied especially intensively and the quality of preservation provides information on the probable notochord and other structures, as well as eye pigmentation, which has engendered vigorous debate on the likely systematic affinities of this enigmatic organism (e.g., Clements et al., 2016; McCoy et al., 2016; 2020; Sallan et al., 2017).

Like the fossil invertebrates and vertebrates, the floral component of the Mazon Creek biota is also diverse (Darrah, 1969; Drinnan and Crane, 1994). It includes plant parts of lycopsids, sphenopsids, ferns, pteridosperms, cordaites, as well as fossils of uncertain relationship. The fossil assemblage is dominated by leaves of ferns, sphenopsids, and pteridosperms (Locatelli et al., 2016), with lycopsids as secondary contributors (Wittry, 2006; 2020). Fossil plants in the Mazon Creek sideritic concretions exhibit excellent 3D morphology but most studies of plants from these nodules have focused on their appearance in two-dimensions and what can be seen on the surfaces of casts and molds. The first plant fossil from the Mazon Creek flora to be reconstructed in 3D was Stephanospermum konopeonus Langford, a medullosan pteridosperm ovule (Drinnan et al., 1990). Using a combination of longitudinal splitting, transverse cutting, serial sectioning and peels, Drinnan et al. (1990) characterized the histology of the ovule and reconstructed its three-dimensional form. Advanced imaging techniques including  $\mu CT$  now provide the opportunity to conduct similar studies non-destructively and more efficiently (Sutton, 2008), but despite the recent widespread use of μCT for reconstructing the anatomy and systematics of Mesozoic and Cenozoic plants (e.g., Friis et al., 2007; 2014; Smith et al., 2009a; Smith et al., 2009b; Collinson et al., 2013; 2016; Manchester et al., 2019; 2022; Matsunaga et al., 2019; 2021; Shi et al., 2021; Smith et al., 2021), this state-of-the-art technology has been barely applied to Mazon Creek plant fossils. To our knowledge, the only Mazon Creek plant that has been studied using a combination of light microscopy and  $\mu$ CT scanning is the medullosan pteridosperm ovule *Stephanospermum braidwoodensis* Spencer et Hilton (Spencer et al., 2013), which is very similar to *Stephanospermum konopeonus*.

Here, we apply these, and other advanced visualization techniques to exceptionally well-preserved fossils of *Tetraphyllostrobus* Gao et Zodrow and *Crossotheca* Zeiller from the Mazon Creek flora to determine their structure and elucidate general principles for the study of Mazon Creek fossil plants using  $\mu$ CT scanning.

### 2 Materials and methods

The Mazon Creek fossil specimens studied here are housed in the paleobotanical collections of the Field Museum (FM). Three specimens recently identified as cf. *Tetraphyllostrobus broganensis* in Mazon Creek siderite nodules (Wittry, 2020) were examined in this study. Two (PP54628, PP58471) were scanned using a GE dual tube  $\mu$ CT scanner at the PaleoCT lab in the Department of Organismal Biology and Anatomy at the University of Chicago. The third (PP34514) was scanned using a Nikon XT H 225ST industrial  $\mu$ CT system with a Perkin Elmer 1620 X-ray detector panel and a tungsten reflection target at the University of Michigan, CTEES facility.

For PP54628 (Figure 1) both part and counterpart were scanned together separated by a thin piece of wrapping foam. The scan used a 240 kV micro-focus tube at 150kV and 250  $\,\mu A$  at 500 m exposure timing, using filter of 0.5 mm Cu. Resolution of voxel x=y=z= 31.8520 µm with 1,200 projection images was achieved. For PP5847 (Figure 2) both part and counterpart were scanned as for PP54628, but a with 180 kV nano-focus tube at 150kV and 250  $\,\mu A$ at 500 m exposure timing, using filter of 0.5 mm Cu. Resolution of voxel x=y=z= 20.8280 µm with 1600 projection images was achieved. PP34514 (Figure 3) was physically sectioned with a Hi-Tech Diamond 6"trim saw. Sections were scanned at 113kV and 105 μA at 500 m exposure timing, using filter of 0.5 mm Cu. Resolution of voxel x=y=z= 12.0 µm with 3,141 projection images was achieved. Anatomical details were obtained from acetate peels (Galtier et al., 1999) taken from the surfaces of individual sections and mounted on slides with Eukitt. Light photographs and microphotographs of acetate peels were obtained at the Field Museum. Macrophotography was with a digital Canon EOS R digital camera (MP-E 65 mm f/2.8 1-5x macro lens) attached to a Stackshot system, with the digital photographs merged using Helicon Focus software. Microphotography was with a ZEISS Axio Imager.A2 microscope using differential interference contrast (DIC) and a Jenoptik Gryphax NAOS digital camera.

The part and counterpart of *Crossotheca* (PP58059; Figure 4) were scanned together as for PP54628 and PP58471, but with a 180 kV nano-focus tube, at 150 kV and 250  $\mu$ A at 500 m exposure timing, using filter of 0.2 mm Cu. Resolution of voxel x=y=z= 32.2230  $\mu$ m with 1,800 projection images was achieved.

The  $\mu$ CT volumes were visualized mainly using Avizo Software 3D 2022.1 (Thermo Fisher Scientific, Waltham, MA, United States). A volume thresholding tool in Avizo was used to demarcate the digitized 3D volume of the fossil specimens from the surrounding matrix of the concretion. Multiple functions were applied to the data

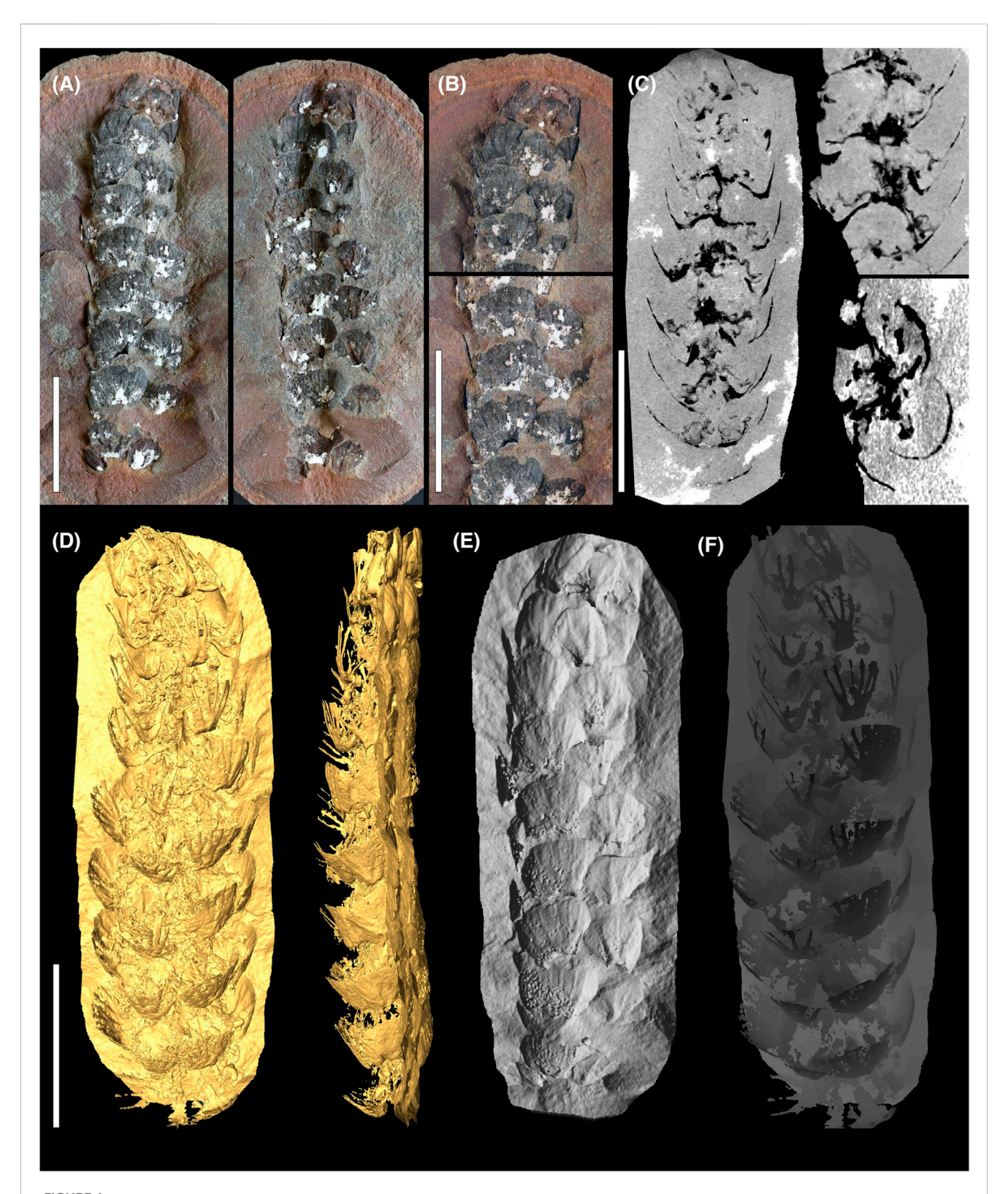


FIGURE 1

Strobilus of cf. Tetraphyllostrobus broganensis (PP54628). (A) Light photographs of part and counterpart of strobilus in a sideritic concretion. (B)
Detail of top and middle portion of strobilus in A (left) showing two orthostichies that suggest a decussate arrangement of the sporophylls. Note the white patches of aluminosilicates on the surface of the strobilus. (C) Computed tomography images showing longitudinal (left and top right) and transverse (bottom right) sections. Note the V-shaped sporophylls in lateral view that are directed downwards proximally and upwards distally, and the curved sporophyll outlines in transverse section. (D) Reflective isosurface renderings showing buried surface of the strobilus in A (left) and a lateral view of that portion of the strobilus embedded in the matrix. Note four of six sporophylls in each apparent whorl which complement the pair of sporophylls visible on the surface in A (left). (E) Surface rendering from A (left) processed with MeshLab (shader: slicingplane) and highlighting the ribbed external surface of (Continued)

### FIGURE 1 (Continued)

sporophylls. **(F)** Surface rendering from D (left) processed with MeshLab (shader: depthmap) showing the four buried sporophylls at each whorl. Scale bars: 10 mm.

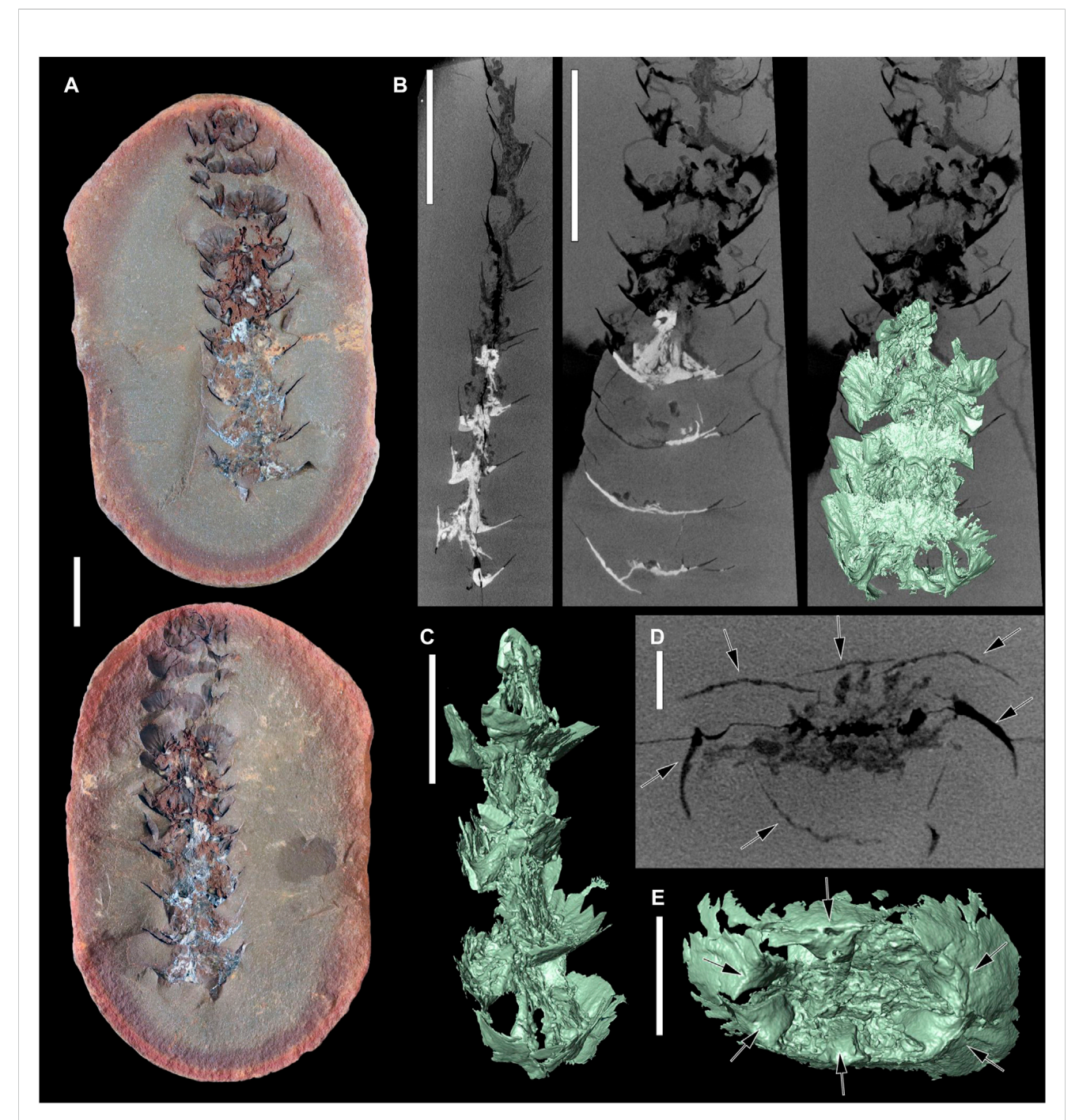
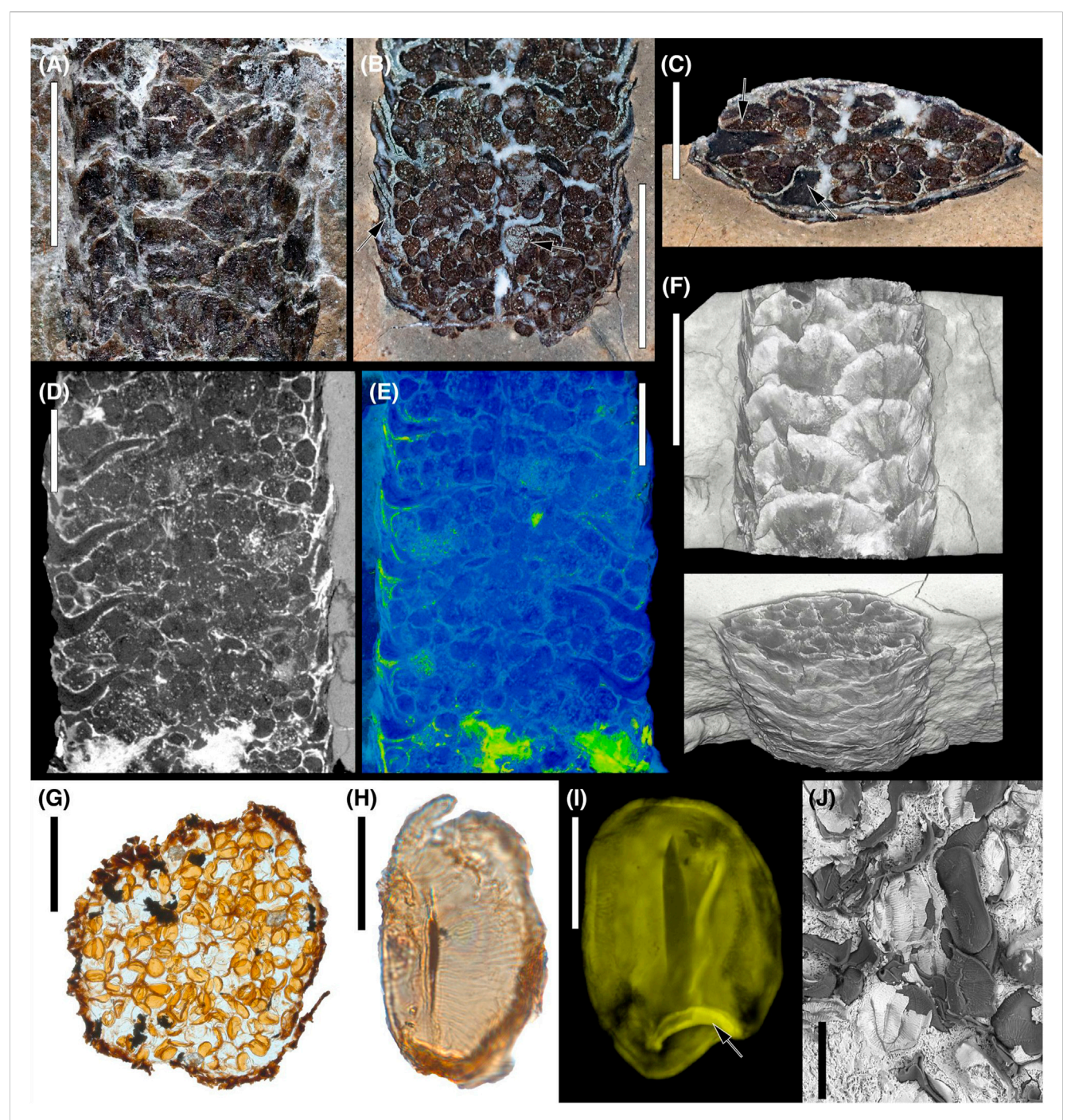


FIGURE 2

Strobilus of cf. *Tetraphyllostrobus broganensis* (PP58471). (A) Light photographs of part and counterpart of strobilus embedded in a sideritic concretion showing the variable mineralogical composition with predominantly iron oxides (upper half) and predominantly sulfide minerals (lower half). (B) Computed tomography images in lateral (left) and frontal (middle, right) sections showing the conspicuous mineralogical transition from predominantly iron oxides (upper half) to sulfide minerals (lower half). Note partial compression of strobilus in left image. Right image shows a superimposed isosurface rendering from the sulfide-rich zone. (C) Isolated isosurface rendering of sulfide-rich zone from B in lateral view showing V-shaped sporophylls in longitudinal section and the separation between successive whorls. (D) Computed tomography image in transverse section showing six sporophylls (arrows). (E) Basal view of surface rendering from C showing the broad proximal shafts of six sporophylls (arrows). Scale bars: 10 mm (A and B); 5 mm (C and E); 2 mm (D).



### FIGURE 3

Strobilus and spores of cf. *Tetraphyllostrobus broganensis* (PP34514). (A) Light photograph of strobilus within sideritic matrix showing two orthostichies that suggest a decussate arrangement of the sporophylls. (B). Light photograph of strobilus in oblique longitudinal section showing spheroidal sporangia (arrows) each containing numerous spores. (C) Light photograph of strobilus in transverse section showing abundant spheroidal sporangia and the broad proximal shafts of two sporophylls (arrows). (D) Computed tomography image in oblique longitudinal section showing the V-shaped sporophylls with broad proximal shafts and numerous spheroidal sporangia. White and bright patches indicate areas of pyritization. (E) Volren image from D showing reflective differential composition of pyrite (light green) *versus* the rest of the strobilus (blue-purple). (F) Volren images in frontal and oblique views from A and C, respectively showing clear orthstichies of overlapping sporophylls. (G) Light micrograph of a peel of an isolated sporangium showing abundant spores. (H) Light micrograph (DIC) of a *Columinisporites* spore showing closely spaced ridges approximately perpendicular to the monolete suture. The longitudinal ridges paralleling the monolete suture are not visible. (I) Airyscan confocal image of monolete *Columinisporites* showing the spore wall, longitudinal monolete suture, very faint perpendicular ridges (left) and longitudinal and oblique folds (arrow) in the spore wall. (J) SEM image of several *Columinisporites* spores showing the characteristic, partially detached, laterally striate perispore. Scale bars: 5 mm (A, B and F); 2 mm (C-E); 200 µm (G); 40 µm (J); 20 µm (H, I).

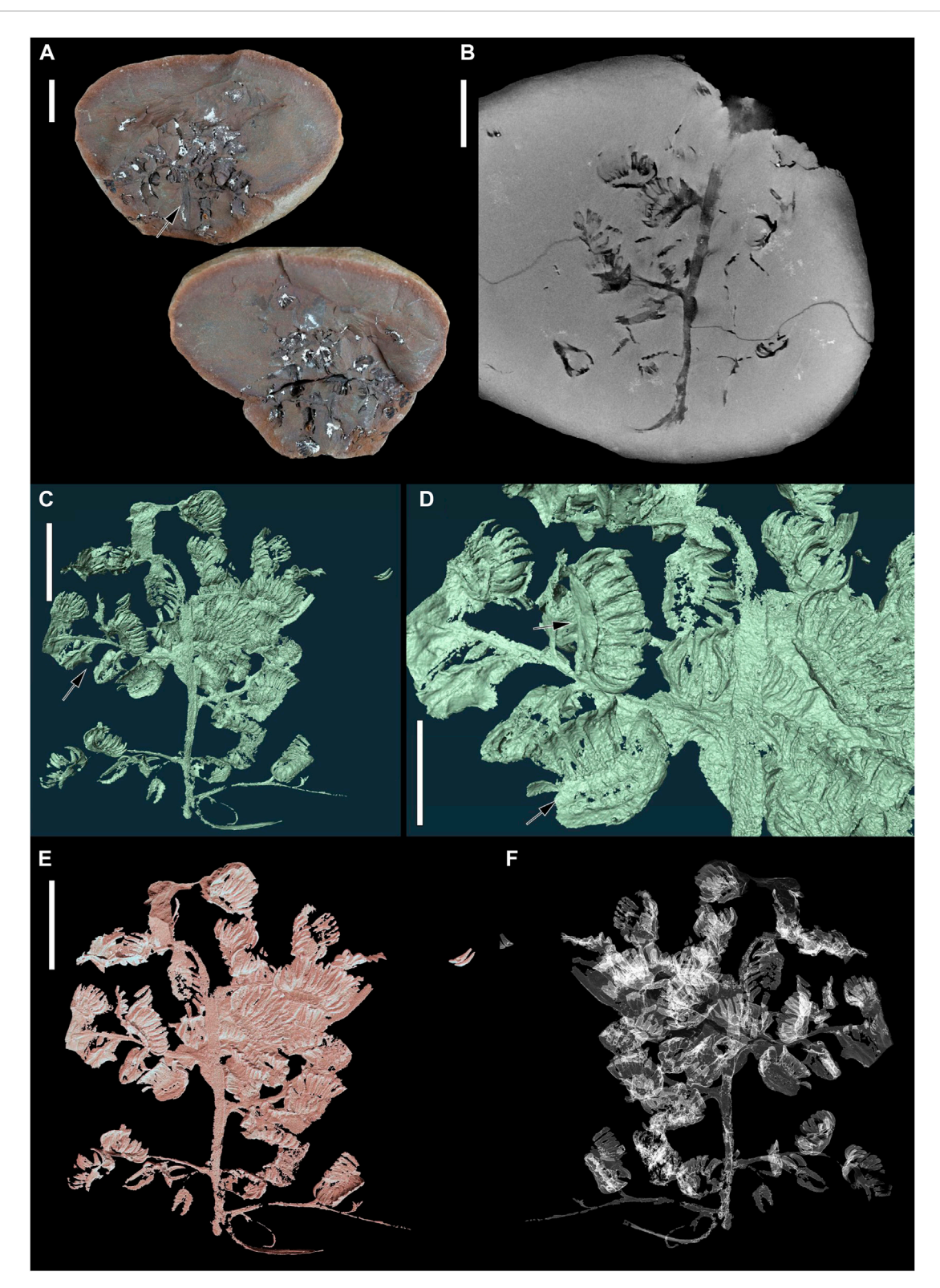


FIGURE 4
Branching axis cf. Crossotheca trisecta (PP58059). (A) Light photographs of part and counterpart in a sideritic concretion. Note the stout central axis (arrow) and white patches of aluminosilicates on surface of the fossil. (B) Computed tomography image showing the stout axis and two secondary axes with attached synangia. (C) Isolated virtual rendering showing the 3D architecture of the branching axis. (D) Detail from C (arrow) showing a synangia in lateral view attached to a simple lamina (upper arrow) and view from below showing the arrangement of the sporangia in two rows (lower arrow). (E) Virtual surface rendering from C processed with MeshLab (shader: radiancescaling, lit sphere effect). (F) Mirror image of virtual cast surface rendering from C processed with MeshLab (shader: x-ray). Scale bars: 10 mm (A, B, C, E and F); 5 mm (D).

to briefly evaluate the quality of the scans and the 3D preservation using volrens, isosurfaces, isosurface renderings, and volume renderings. An isosurface was first created to reconstruct the buried surface of the parts and counterparts (draw style: shaded) with the "back face" function selected. Once the desired surface models were achieved, each volume was exported as a .ply file for further analysis or visualization in MeshLab 2022.02 (Cignoni et al., 2008). Additional filters in MeshLab were helpful for removal of isolated surface fragments. MeshLab rendering-shaders functions, for example, depthmap, slicingplane, radiancescaling (lit-sphere effect), and x-ray were applied to improve the visualization of the surface models.

In-situ spores from the permineralized cone of specimen PP34514 (Figure 3) were examined directly on polished specimens attached to a stub and scanned at the National Museum of Natural History with a Zeiss EVO MA15 scanning electron microscope (EHT = 12 kv, WD = 7.5 mm, I probe = 1.2 nA, signalA = CZBSD). The spores were also imaged using a Zeiss LSM 980 with Airyscan 2 confocal superresolution microscope at the Smithsonian Tropical Research Institute. Images were taken at  $\times$ 630 magnification ( $\times$ 63/NA 1.4 oil DIC) with fluorescence contrast, using 561 and 639 nm laser wavelengths and an intensity of 40% and 16% respectively. A total of 147 axial images were taken at 0.19  $\mu$ m increments to capture the 3D morphology of each spore. Images were analyzed using Zeiss Zen 3.4.

To evaluate the response to  $\mu$ CT of specimens preserved in different minerals we acquired *in situ* and *ex-situ* elemental maps (Oxford Instruments AZTec) of the fossil concretions (Supplementary Material). *In-situ* and *ex-situ* Raman microspectroscopy was performed at FM with a WITec alpha 300 R system equipped with a 532 nm laser (Supplementary Material). Data was analyzed using WITec Project Plus software.

### 2 Results

### 2.1 Tetraphyllostrobus

Since its original description the systematic placement of *Tetraphyllostrobus* has been problematic. The genus was described based on approximately thirty compression specimens from the Late Carboniferous of Canada that were assigned to the only species of the genus, *Tetraphyllostrobus broganensis* Gao and Zodrow (Gao and Zodrow, 1990). The new morphological and anatomical information on the strobili and *in situ* spores of three specimens identified as cf. *Tetraphyllostrobus broganensis* in Mazon Creek siderite nodules (Wittry, 2020) confirms their assignment *Tetraphyllostrobus*. A detailed systematic and nomenclatural treatment of these fossils will be the subject of a separate study.

The three  $\mu$ CT scans of the Mazon Creek specimens of cf. *Tetraphyllostrobus broganensis* (Figures 1–3) all reveal excellent 3D preservation of the strobili. Some compaction of the original plant material is evident, but the visualizations reveal whorls of six sporophylls at each node (Figures 1C, F; Figures 2D, E) rather than pairs of sporophylls in a decussate arrangement, as was initially described based on the compression specimens of *Tetraphyllostrobus* (Gao and Zodrow, 1990). This aspect of the

morphology is best seen in a combination of digital transverse sections (Figure 1C, 2D), isosurface images of the buried surface (Figure 1D), internal depth map visualizations (Figure 1F), and volume renderings (Figures 2B, C, E). The  $\mu$ CT data from all three strobili also show that each sporophyll has a V-shaped appearance in longitudinal section (Figures 1C, 2B, 3D). This results from the downward orientation of the proximal sporophyll stalk at an angle of ca. 45°, with the distal lamina then turned prominently upwards. The seemingly decussate organization of the sporophylls noted in compression fossils (Gao and Zodrow, 1990) is also apparent in the Mazon Creek specimens (Wittry, 2020) as two distinct orthostichies. This is a result of the facture plane that passes across the surface of the cone clearly exposing only two of the six sporophylls in each whorl (e.g., Figure 2B, left).

Specimen PP34514 shows excellent preservation of sporangia, which are well seen in both longitudinal and transverse sections (Figures 3B-E, G-J). DIC microscopy, Airyscan, and SEM all show that the spores in specimen PP34514 are attributable to the Carboniferous dispersed spore genus Columinisporites (Figures 3G-J) (Peppers, 1964). Isolated Columinisporites spores have been found in late Pennsylvanian deposits across the Illinois basin (Peppers, 1964; 1970), but this is the first in situ record in the Mazon Creek flora. The genus was described as an elliptical to reniform spore with sculpture characterized by several to numerous prominent ridges running roughly parallel to the long axis of the spore and a network of smaller (secondary) ridges extending approximately transverse to the longitudinal ridges (Peppers, 1964). This distinctive sculpture is in a layer external to the spore wall that is readily detached and is generally interpreted as a perispore (Taylor, 1986). Perispore remnants often remain attached to the spore wall.

The proximal monolete aperture is clearly visible with DIC and Airyscan imaging (Figures 3H, I). DIC also resolves the anastomosing network of transverse secondary ridges on the spore wall, although the primary ridges are not visible (Figure 3H). In the Airyscan images this transverse ornamentation is barely noticeable but a two-layered spore wall is visible (Figure 3I). SEM is the most effective for demonstrating the longitudinal ridges (visible as grooves in the micrograph) as well as the monolete apertures and secondary ridges (Figure 3J). SEM also clearly illustrates the detachable nature of the perispore, showing some portions embedded within the tissue of the sporangium and other portions adhering to the spore wall. Primary ridges appear as grooves, indicating that they are in negative relief, that is, the underside of the perispore is imaged. These observations support interpretations that view the perispore was derived from tapetal tissue as in modern ferns and sphenopsids (Wallace et al., 2011). The marked contrast in the SEM image between the spore wall (dark) and the perispore and embedding tissue (light) also points to compositional differences between the sporopollenin exine and the presumed tapetally-derived perisporial tissues.

### 2.2 Crossotheca

Crossotheca includes over a dozen described species of microsporangiate fertile units (Taylor et al., 2009; McLoughlin, 2021) that have been interpreted both as a lyginopterid pollen

organ (Sellards, 1902; Darrah, 1937; Andrews and Mamay, 1948; Millay and Taylor, 1979) and the fertile frond of a eusporangiate fern (Danzé, 1955; Brousmiche, 1982).

The µCT scan of the nodule of cf. Crossotheca trisecta (Sellards, 1902; Wittry, 2020) provides an excellent illustration of the utility of combining digital sections (Figure 4B), virtual cast surface renderings (Figures 4C, D) with Meshlab processing (Figures 4E, F) for reconstructing complex 3D plant parts such as Crossotheca. The specimen is mainly preserved as a mold with some organic material remaining along the synangia walls (Figure 4A). This style of preservation allowed almost instantaneous reproduction of a virtual cast surface rendering, which is less time-consuming, and likely more accurate, than manual and interpretative standard segmentation techniques. The virtual cast surface renderings and MeshLab (Figures 4C-F) visualizations also reveal detailed external and internal morphological features of the synangia that are not clearly visible on the uneven surfaces of the concretion with standard reflected light microscopy (Figure 4D). Additional µCT scans of other Crossotheca specimens will be needed for more detailed assessment of the systematic affinities of these fertile units but the results presented here illustrate the potential of µCT scanning for the efficient analysis of the 3D structure in Crossotheca and similar specimens with complex morphologies from the Mazon Creek Lagerstätte.

# 2.3 Mineralogy of Mazon Creek plant concretions and computed tomography visualization

A recent study (Cotroneo et al., 2016), and the SEM chemical maps and *in situ* and *ex-situ* Raman microspectroscopy results presented here, confirm that the non-fossiliferous part of Mazon Creek concretions is mainly sideritic in composition, as has long been recognized. The four specimens analyzed reveal that the plant fossils often preserve a high-fidelity impression of their external surface, with the resulting void created by the loss of the original plant material infilled by various minerals that precipitate in the space. Based on these results, we group the minerals involved in a similar manner to Cotroneo et al. (2016) (Supplementary Material): 1) replacement by calcite and aluminosilicates (likely kaolinite, illite), 2) replacement by iron oxides, 3) replacement by sulfide minerals (e.g., sphalerite), and 4) pyritization with silicates and calcite present (Supplementary Table S1).

The three concretions containing *Tetraphyllostrobus* show that infilling minerals can either facilitate or obscure  $\mu$ CT visualization and 3D reconstruction of the original plant organ. In  $\mu$ CT images of strobilus PP54628 (Figure 1) mainly shows organic exterior walls with abundant aluminosilicates, which are visible as white patches on the surface of both part and counterpart of the concretion or bright areas with poor resolution (e.g., scattering artifacts) (Figure 1C). The organic exterior walls of the strobilus also display sufficient contrast for easy visualization in  $\mu$ CT images resulting in correspondingly less time-consuming and more straightforward renderings of complex 3D morphology (Figures 1D–F) than manual and exhaustive standard segmentation techniques (e.g., Matsunaga et al., 2021; Herrera et al., 2022).

Strobilus PP58471 (Figure 2) preserves thinner organic exterior walls than PP54628 (Figure 1), but there are distinct mineralogical domains in the upper and lower halves of the specimen. The upper half is mainly replaced by iron oxides while the lower portion is replaced mainly by sulfides (i.e., sphalerite). Other areas are empty, perhaps due to loss of the mineral infilling when the concretion was split or no infiltration of precipitates, for example, near the tips of the sporophylls. Both mineralogical domains (Figures 2B, D) exhibit good contrast in  $\mu$ CT images, but sulfides gave better conditions for creating and rapidly isolating 3D renderings using different volume threshold values and tools (Figures 2C, E).

Strobilus PP34514 (Figure 3) shows the greatest mineralogical diversity of the three Tetraphyllostrobus concretions. The central axis and sporophylls are primarily organic, whereas the sporangia appear filled with calcite and silicates. This specimen also presents various degrees of pyritization along the walls of the axis, sporophylls and sporangia, and there are also small pyrite crystals scattered throughout the strobilus. White patches of calcite crystals also fill the empty spaces in the strobilus and sporophylls, and also between sporangia. Overall, the predominantly organic nature of the strobilus provides good contrast in µCT images, but scattered pyritization results in disruptive scattering artifacts (Figure 3D). However, where small pyrite crystals occur along the edges of morphological features, they become helpful in recognizing sporophylls and sporangia in volren images (Figure 3E).

The branching system of cf. Crossotheca trisecta (PP58059) (Figure 4) is mainly preserved as a mold with some organic material remaining along the central axis and the walls of the synangia. The μCT images and renderings show excellent 3D preservation and minimal compressional deformation of synangia. As in the Tetraphyllostrobus strobilus PP54628 (Figure 1), white patches of aluminosilicates result in low resolution and poor contrast in CT images. However, the 3D preservation as a mold yields a high-fidelity impression of the external surface of the original plant organ facilitating the 3D rendering and isolation of the specimen from the sideritic matrix (Figures 4C, D). The surface models obtained with MeshLab (Figures 4E, F) also show the utility of 3D mesh processing software for visualizing complex 3D structures.

### 3 Discussion

Biomarkers and macromolecular biosignatures obtained with *in situ* Raman spectra studies on vertebrates, invertebrates, and coprolites from Mazon Creek have recently provided exciting results for reevaluating the affinity of problematic fossil organisms (McCoy et al., 2020) and the reconstruction of trophic relationships in this Carboniferous ecosystem (Tripp et al., 2022). Raman analyses showed the potential utility of this technique for recognizing the mineralogical composition of Mazon Creek fossil plants, but future biomarker analyses could also help elucidate the deep relationships among vascular plants and other unexplored trophic plant dynamic processes.

Approximately eighty plant taxa have been recognized from the Mazon Creek Lagerstätte, and there are more than 20,000 plant fossil specimens in the Field Museum collections. However, many of the plant taxa require careful structural analysis and systematic revaluation, including the specimens of Tetraphyllostrobus and Crossotheca studied here. A previous study by Drinnan et al. (1990) on ovules of Stephanospermum konopeonus demonstrated the potential for extracting high quality 3D information from plant fossils preserved in Mazon Creek ovules. More recently a study by Spencer et al. (2013) on a similar medullosan ovule, Stephanospermum braidwoodensis, showed that non-destructive μCT further enhanced the opportunities to develop 3D reconstructions of fossil plants preserved in siderite nodules. The current study on other kinds of plant fossils in Mazon Creek nodules further demonstrates the value of µCT scanning and the resulting visualizations for understanding the 3D structure of Paleozoic plants. However, the quality of results will be influenced by the composition of the minerals filling the voids left by the decomposing plant material, with calcite, aluminosilicates, iron oxides, sulfides, and pyrite all potentially involved. For 3D renderings of Mazon Creek plants, specimens with high amounts of organic preservation and more homogeneous mineralization should be prioritized, with sulfides preferred over iron oxides. Specimens in which the voids are filled in part by aluminosilicates are likely to give the least helpful results. Excellent preservation of spores studied with DIC, SEM, and Airyscan confocal super-resolution microscopy also provides useful high-quality information for the correct identification of in situ palynomorphs.

# Data availability statement

The raw data supporting the conclusions of this article will be made available by the authors, without undue reservation.

### **Author contributions**

FH designed the outline of this work. PRC initially studied and prepared specimen PP34514. FH, CLH, SYS, PAL, AIN, and MPD processed  $\mu$ CT, SEM, and Airyscan data. JW identified fossil specimens. FH, YZ, and PRH obtained elemental maps and conducted Raman microspectroscopy. FH wrote the manuscript and discussed the contents with CLH, SYS, PAL, AIN, JW, YZ, PRH, PRC, and MPD. All authors contributed to the article and approved the submitted version.

### References

Andrews, H. N., and Mamay, S. A. (1948). A *Crossotheca* from northern Illinois. *Ann. Mo. Bot. Gard.* 35 (3), 203–205. doi:10.2307/2394529

Baird, G. C., Shabica, C. W., Anderson, J. L., and Richardson, E. S., Jr. (1985). Biota of a Pennsylvanian muddy coast: Habitats within the Mazonian delta complex, northeast Illinois. *J. Paleontol.* 59 (2), 253–281.

Baird, G. C., Sroka, S. D., Shabica, C. W., and Kuecher, G. J. (1986). Taphonomy of middle Pennsylvanian Mazon Creek area fossil localities, northeast Illinois: Significance of exceptional fossil preservation in syngenetic concretions. *Palaios* 1, 271–285. doi:10.2307/3514690

# **Funding**

This work was funded by the Negaunee Integrative Research Center (to FH, MPD, and PRH) A. Susman (to FH), and the NSF grant 1802352 (The Pteridological Collections Consortium: An integrative approach to pteridophyte diversity over the last 420 million years) for the digitization of the Mazon Creek Flora at the Field Museum. MPD was supported by the Negaunee Integrative Postdoctoral Scientist Fellowship, Field Museum of Natural History.

# Acknowledgments

The authors would like to thank Carlos Jaramillo at the Smithsonian Tropical Research Institute for providing the Airyscan confocal microscope and Zhe-Xi Luo for assistance with micro-CT scanning at University of Chicago. This study includes data produced in the CTEES facility at University of Michigan, supported by the Department of Earth and Environmental Sciences and College of Literature, Science, and the Arts. The authors would also like to thank Akiko Shinya and reviewers for their helpful comments.

### Conflict of interest

The authors declare that the research was conducted in the absence of any commercial or financial relationships that could be construed as a potential conflict of interest.

### Publisher's note

All claims expressed in this article are solely those of the authors and do not necessarily represent those of their affiliated organizations, or those of the publisher, the editors and the reviewers. Any product that may be evaluated in this article, or claim that may be made by its manufacturer, is not guaranteed or endorsed by the publisher.

# Supplementary material

The Supplementary Material for this article can be found online at: https://www.frontiersin.org/articles/10.3389/feart.2023.1200976/full#supplementary-material

Brousmiche, C. (1982). Sur la synonymie de *Crossotheca boulayi* Zeiller, 1886–88 et *Crossotheca bourozii* Danzé, 1956 avec l'espéce-type du genre: *Crossotheca crepinii* Zeiller, 1883: Une nouvelle interprétation de la fructification. *Geobios* 15 (5), 679–703. doi:10.1016/S00166995(82)80002-8

Cignoni, P., Callieri, M., Corsini, M., Dellepiane, M., Ganovelli, F., and Ranzuglia, G. (2008). *MeshLab: An open-source mesh processing tool* in Sixth Eurographics Italian Chapter Conference, Salerno, Italy, July 2nd - 4th, 2008, 129–136.

Clements, T., Dolocan, A., Martin, P., Purnell, M., Vinther, J., and Gabbott, S. E. (2016). The eyes of *Tullimonstrum* reveal a vertebrate affinity. *Nature* 532, 500–503. doi:10.1038/nature17647

Clements, T., Purnell, M., and Gabbott, S. (2019). The Mazon Creek Lagerstätte: A diverse late Paleozoic ecosystem entombed within siderite concretions. *J. Geol. Soc.* 176 (1), 1–11. doi:10.1144/jgs2018-088

Collinson, M. E., Smith, S. Y., van Konijnenburg-van Cittert, J. H., Batten, D. J., van der Burgh, J., Barke, J., et al. (2013). New observations and synthesis of Paleogene heterosporous water ferns. *Int. J. Plant Sci.* 174 (3), 350–363. doi:10. 1086/668249

Collinson, M. E., Adams, N. F., Manchester, S. R., Stull, G. W., Herrera, F., Smith, S. Y., et al. (2016). X-Ray micro-computed tomography (micro-CT) of pyrite-permineralized fruits and seeds from the London Clay Formation (Ypresian) conserved in silicone oil: A critical evaluation. *Botany* 94 (9), 697–711. doi:10.1139/cjb-2016-0078

Cotroneo, S., Schiffbauer, J., McCoy, V., Wortmann, U., Darroch, S., Peng, Y., et al. (2016). A new model of the formation of Pennsylvanian iron carbonate concretions hosting exceptional soft-bodied fossils in Mazon Creek, Illinois. *Geobiology* 14 (6), 543–555. doi:10.1111/gbi.12197

Danzé, J. (1955). Le genre Crossotheca Zeiller C. R. Aci. Sc. 241, 1616-1618.

Darrah, W. C. (1937). Codonotheca and Crossotheca: Polliniferous structures of pteridosperms. Bot. Mus. Lealf. Harv. Univ. 4 (9), 153–172. doi:10.5962/p.295102

Darrah, W. C. (1969). A critical review of the Upper Pennsylvanian floras of eastern United States with notes on the Mazon Creek flora of Illinois. Gettysburg, PA, USA: Privately published, 220.

Drinnan, A. N., Schramke, J. M., and Crane, P. R. (1990). Stephanospermum konopeonus (Langford) Comb. Nov.: A medullosan ovule from the middle Pennsylvanian Mazon Creek flora of northeastern Illinois, USA. Bot. Gaz. 151 (3), 385–401. doi:10.1086/337839

Drinnan, A. N., and Crane, P. R. (1994). A synopsis of medullosan pollen organs from the middle Pennsylvanian Mazon Creek flora of northeastern Illinois, USA. *Rev. Palaeobot. Palynol.* 80 (3-4), 235–257. doi:10.1016/0034-6667(94)90003-5

Friis, E. M., Crane, P. R., Pedersen, K. R., Bengtson, S., Donoghue, P. C., Grimm, G. W., et al. (2007). Phase-contrast X-ray microtomography links Cretaceous seeds with Gnetales and Bennettitales. *Nature* 450 (7169), 549–552. doi:10.1038/nature06278

Friis, E. M., Marone, F., Pedersen, K. R., Crane, P. R., and Stampanoni, M. (2014). Three-dimensional visualization of fossil flowers, fruits, seeds, and other plant remains using synchrotron radiation X-ray tomographic microscopy (SRXTM): New insights into Cretaceous plant diversity. *J. Paleontol.* 88 (4), 684–701. doi:10.1666/13-099

Galtier, J., Phillips, T. L., Jones, T. P., and Rowe, N. P. (1999). The acetate peel technique" in Fossil plants and spores: Modern techniques. Editors T. P. Jones and N. P. Rowe (London: Geological Society of London), 67–70.

Gao, Z., and Zodrow, E. L. (1990). A new strobilus *Tetraphyllostrobus broganensis* gen. et sp. nov. from the Upper Carboniferous, Sydney Coalfield, Nova Scotia, Canada. *Rev. Palaeobot. Palynol.* 66 (1-2), 3–11. doi:10.1016/0034-6667(90)90025-E

Herrera, F., Testo, W. L., Field, A. R., Clark, E. G., Herendeen, P. S., Crane, P. R., et al. (2022). A permineralized Early Cretaceous lycopsid from China and the evolution of crown clubmosses. *New Phyto.* 233, 2310–2322. doi:10.1111/nph.17874

Johnson, R. G., and Richardson, E. S., Jr (1966). A remarkable Pennsylvanian fauna from the Mazon Creek area, Illinois. J. Geol. 74, 626–631. doi:10.1086/627194

Locatelli, E. R., Krajewski, L., Chochinov, A. V., and Laflamme, M. (2016). Taphonomic variance between marattialean ferns and medullosan seed ferns in the Carboniferous Mazon Creek Lagerstätte, Illinois, USA. *Palaios* 31 (3), 97–110. doi:10. 2110/palo.2015.073

Manchester, S. R., Kapgate, D. K., Ramteke, D. D., Patil, S. P., and Smith, S. Y. (2019). Morphology and anatomy of the angiosperm fruit *Baccatocarpon*, incertae sedis, from the Maastrichtian Deccan Intertrappean Beds of India. *Acta Palaeobot*. 59 (2), 241–250. doi:10.2478/acpa-2019-0019

Manchester, S. R., Zhang, X., Hotton, C. L., Wing, S., and Crane, P. R. (2022). Two-seeded cones of probable gnetalean affinity from the Morrison Formation (Late Jurassic) of Utah and Colorado, USA. *Acta Palaeob*. 62 (2), 77–92. doi:10.35535/acpa-2022-0006

Matsunaga, K. K. S., Herendeen, P. S., Herrera, F., Ichinnorov, N., Crane, P. R., and Shi, G. (2021). Ovulate cones of *Schizolepidopsis ediae* sp. nov. provide insights into the evolution of Pinaceae. *Int. J. Plant Sci.* 182 (6), 490–507. doi:10.1086/714281

Matsunaga, K. K. S., Manchester, S. R., Srivastava, R., Kapgate, D. K., and Smith, S. Y. (2019). Fossil palm fruits from India indicate a Cretaceous origin of Arecaceae tribe Borasseae. *Bot. J. Linn. Soc.* 190 (3), 260–280. doi:10.1093/botlinnean/boz019

McCoy, V. E., Saupe, E. E., Lamsdell, J. C., Tarhan, L. G., McMahon, S., Lidgard, S., et al. (2016). The 'Tully monster' is a vertebrate. *Nature* 532, 496–499. doi:10.1038/nature16992

McCoy, V. E., Wiemann, J., Lamsdell, J. C., Whalen, C. D., Lidgard, S., Mayer, P., et al. (2020). Chemical signatures of soft tissues distinguish between vertebrates and invertebrates from the Carboniferous Mazon Creek Lagerstätte of Illinois. *Geobiology* 00, 560–565. doi:10.1111/gbi.12397

McLoughlin, S. (2021). *Gymnosperms*" in Encyclopedia of Geology. Editors D. Alderton and S. A. Elias Second Edition (Cambridge: Academic Press), 476–500. doi:10.1016/B978-0-08-102908-4.00068-0

Millay, M. A., and Taylor, T. N. (1979). Paleozoic seed fern pollen organs. *Bot. Rev.* 45, 301–375. doi:10.1007/BF02860858

Nitecki, M. H. (1979). in Mazon Creek fauna and flora: A hundred years of investigation" in Mazon Creek fossils. Editor M. H. Nitecki (New York: Academic Press), 1–12.

Peppers, R. A. (1964). Spores in strata of late Pennsylvanian cyclothems in the Illinois basin. *Ill. State Geol. Surv. Bull.* 90, 1–89.

Peppers, R. A. (1970). Correlation and palynology of coals in the Carbondale and Spoon Formations (Pennsylvanian) of the northeastern part of the Illinois basin. *Ill. State Geol. Surv. Bull.* 93, 1–173.

Richardson, E. S., Jr (1966). Wormlike fossil from the Pennsylvanian of Illinois. Science 151 (3706), 75–76. doi:10.1126/science.151.3706.75.b

Sallan, L., Giles, S., Sansom, R. S., Clarke, J. T., Johanson, Z., Sansom, I. J., et al. (2017). The 'Tully Monster' is not a vertebrate: Characters, convergence and taphonomy in Palaeozoic problematic animals. *Palaeontology* 60 (2), 149–157. doi:10.1111/pala.12282

Sellards, E. H. (1902). On the fertile fronds of *Crossotheca* and *Myriotheca*, and on the spores of other Carboniferous ferns from Mazon Creek, Illinois. *Am. J. Sci.* 14 (81), 195–202. doi:10.2475/ais.s4-14.81.195

Shi, G., Herrera, F., Herendeen, P. S., Clark, E. G., and Crane, P. R. (2021). Mesozoic cupules and the origin of the angiosperm second integument. *Nature* 594 (7862), 223–226. doi:10.1038/s41586-021-03598-w

Smith, S. Y., Collinson, M. E., Rudall, P. J., Simpson, D. A., Marone, F., and Stampanoni, M. (2009a). Virtual taphonomy using synchrotron tomographic microscopy reveals cryptic features and internal structure of modern and fossil plants. *Proc. Natl. Acad. Sci. U. S. A.* 106 (29), 12013–12018. doi:10.1073/pnas. 0901468106

Smith, S. Y., Collinson, M. E., Simpson, D. A., Rudall, P. J., Marone, F., and Stampanoni, M. (2009b). Elucidating the affinities and habitat of ancient, widespread Cyperaceae: *Volkeria messelensis* gen. et sp. nov., a fossil mapanioid sedge from the Eocene of Europe. *Am. J. Bot.* 96 (8), 1506–1518. doi:10.3732/ajb. 0800427

Smith, S. Y., Kapgate, D. K., Robinson, S., Srivastava, R., Benedict, J. C., and Manchester, S. R. (2021). Fossil fruits and seeds of Zingiberales from the late Cretaceous—early Cenozoic Deccan Intertrappean Beds of India. *Int. J. Plant Sci.* 182 (2), 91–108. doi:10.1086/711474

Spencer, A. R. T., Hilton, J., and Sutton, M. D. (2013). Combined methodologies for three-dimensional reconstruction of fossil plants preserved in siderite nodules: *Stephanospermum braidwoodensis* nov. sp. (Medullosales) from the Mazon Creek Lagerstätte. *Rev. Palaeobot. Palynol.* 188, 1–17. doi:10.1016/j.revpalbo.2012. 09 001

Sutton, M. D. (2008). Tomographic techniques for the study of exceptionally preserved fossils. *Proc. R. Soc. B* 275 (1643), 1587–1593. doi:10.1098/rspb.2008.

Taylor, E. L., Taylor, T. N., and Krings, M. (2009). Paleobotany: The biology and evolution of fossil plants. Burlington, Massachusetts: Academic Press.

Taylor, W. A. (1986). Ultrastructure of sphenophyllalean spores. *Rev. Palaeobot. Palynol.* 47 (1–2), 105–128. doi:10.1016/0034-6667(86)90009-6

Tripp, M., Wiemann, J., Brocks, J., Mayer, P., Schwark, L., and Grice, K. (2022). Fossil biomarkers and biosignatures preserved in coprolites reveal carnivorous diets in the Carboniferous Mazon Creek ecosystem. *Biology* 1289, 1289. doi:10.3390/biology11091289

Wallace, S., Fleming, A., Wellman, C. H., and Beerling, D. J. (2011). Evolutionary development of the plant and spore wall. *AoB Plants* plr027, plr027. doi:10.1093/aobpla/plr027

Wittry, J. (2006). The Mazon Creek fossil flora. Illinois, USA: Earth Science Club of Northern Illinois, 164.

Wittry, J. (2020). A comprehensive guide to the fossil flora of Mazon Creek. Illinois, USA: Earth Science Club of Northern Illinois, 275.